J Solid State Electrochem (2004) 8: 892–899
DOI 10.1007/s10008-004-0517-x

ORIGINAL PAPER

G. Stalnionis · L. Tamašauskaitė-Tamašiūnaitė
V. Pautienienė · A. Sudavičius · Z. Jusys

# Modification of a Pt surface by spontaneous Sn deposition for electrocatalytic applications

## 1. Catalyst preparation and characterization

Received: 19 December 2003 / Accepted: 3 February 2004 / Published online: 23 March 2004


**Abstract** In the present communication we explored a simple "dip-coating" method for spontaneous (without applying an external current or additional reducing agents) modification of Pt surface by both tin oxy-species and tin metal based on hydrolysis of tin chloride complex and autocatalytic (electroless) deposition of tin for fabrication of the fuel cell catalysts with improved CO tolerance. It consisted of (i) Pt immersion into $SnCl_2$/HCl solution under open-circuit conditions; (ii) subsequent rinsing of the surface by pure water. The resulting Sn-modified Pt surfaces were characterized by atomic force microscopy (AFM), X-ray photoelectron spectroscopy (XPS) and cyclic voltammetry (CV). Two types of tin species, namely, tin oxide/hydroxide species and metallic tin were identified at Pt surface. Tin oxide/hydroxide species were assumed to be derived as a result of Sn(II) chloride complex hydrolysis, while tin metal particles were most likely deposited spontaneously on Pt surface due to disproportionation of Sn(II) to Sn(IV) and metallic tin, competing with dissolution of the Sn deposit in strongly acidic medium. Modifying tin species show a satisfactory stability in 0.5-M $H_2SO_4$ solution at potentials relevant to low-temperature fuel cell operating conditions (below 0.6 V vs. a standard hydrogen electrode, SHE).

**Keywords** Spontaneous deposition · Surface modification · Tin · Pt · AFM · XPS · Electrocatalysis

G. Stalnionis · L. Tamašauskaitė-Tamašiūnaitė
V. Pautienienė · A. Sudavičius · Z. Jusys (✉)
Institute of Chemistry, A. Goštauto 9, 2600 Vilnius, Lithuania
E-mail: zenonas.jusys@chemie.uni-ulm.de
Tel.: +49-731-502-5454
Fax: +49-731-502-5452

*Present address:* Z. Jusys
Department of Surface Chemistry and Catalysis,
University of Ulm, Albert-Einstein-Allee 47,
89069 Ulm, Germany

## Introduction

The CO tolerance of the anode catalysts for low-temperature polymer electrolyte membrane fuel cell (PEMFC) applications can be markedly improved by combining Pt with a less-noble metal component, allowing oxidation of poisoning $CO_{ad}$ species on Pt sites in surface reaction with OH, electrosorbed on oxophilic metal sites at lower overpotentials compared to Pt—the latter reaction sequence is usually referred to as a bifunctional mechanism [1, 2]. This stimulated tremendous efforts (both experimental and theoretical) in formulation of novel PEMFC catalyst materials with an improved performance (e.g., see a recent review [3] and references cited therein). The most promising compositions for electrocatalytic applications up to now are Ru, Os, Ir, Sn, Bi, Mo, V, W, Re etc. binary (or ternary/quaternary [4, 5, 6]) combinations with Pt. These can be divided into two major groups with respect to the catalyst preparation/composition, i.e., (i) bimetallic alloys and (ii) surface-modified catalysts.

The first group deals with metal alloys, ensuring an intimate intermixing of the constituent atoms and uniform chemical and structural (in the case of single crystals) long-range composition. Electrochemically deposited [7, 8, 9, 10, 11, 12, 13, 14] or chemically formed [15, 16, 17, 18, 19, 20] bimetallic alloys (including nano-structured catalysts), sputter-deposited alloys [21, 22, 23], well-characterized metallurgic alloys [3, 24, 25, 26, 27, 28, 29, 30], and, finally, single crystal (surface)alloy electrodes [31, 32] were extensively studied in PEMFC-related electrocatalytic reactions to achieve important kinetic and mechanistic insights about the relation between composition (structure) and the activity of these surfaces.

The other approach (besides alloying) used to improve the CO tolerance of Pt electrocatalyst is Pt surface modification by oxophilic metals. The latter can be achieved by (i) underpotential deposition (UPD) and electrodeposition of (sub)monolayers of metal, e.g., tin,

on the Pt surface [33, 34, 35, 36, 37, 38, 39, 40, 41, 42, 43, 44, 45, 46, 47], including step-decoration of single crystal surfaces [48, 49]; (ii) physicochemical deposition of modifying metal through an organometallic route (thermal decomposition of organyl complexes of non-noble metals on Pt surface) [50, 51, 52], photolithography [53], ion implantation [54], or epitaxially grown overlayers under ultrahigh vacuum conditions [55, 56]; (iii) surface modification through "spontaneous deposition"—adsorption of metal complexes on Pt surface and a subsequent electrochemical reduction of the precursor, or direct electrodeposition of submonolayer amounts of modifying metal on Pt substrate [57, 58, 59, 60, 61, 62, 63]. The third route is used most often for modification of Pt surfaces (polycrystalline, single crystal and nanoparticle) by Ru and Os, while the first and second are used for modification of the Pt surface by Sn, Ge, Ru, etc.

In the present communication we explore a "dip-coating" approach for spontaneous Pt surface modification through deposition of tin and tin oxy-species. The notable difference from the spontaneous deposition method, developed by Wieckowski et al. for Pt modification by Ru [53, 54], and tin-UPD method [33, 34, 35, 36, 37, 38, 39, 40, 41, 42, 43, 44, 45, 46, 47], is that this approach is a simple *non-electrochemical* way (without applying an external current or additional reducing agent during and after modification) for modification of Pt surface by tin species. Our approach is similar to the ill-characterized spontaneous tin deposition procedure performed on Pt surfaces under open-circuit conditions introduced earlier [64, 65]. The approach we developed has major advantages over the organometallic route [50, 51, 52], since controlled modification of Pt surface by Sn species is achieved at ambient temperature from aqueous solutions. Moreover, our method can be easily adopted and used for Sn-modification of solid Pt model electrode surfaces as well as for realistic Pt nano-particle fuel cell catalysts [65, 66] or carbon support [67].

In the following, after a brief description of the modification procedure and experimental details, we will present the characterization of tin-modified polycrystalline Pt by means of atomic force microscopy (AFM), X-ray photoelectron spectroscopy (XPS) and cyclic voltammetry (CV) and discuss possible pathways of the modification process. The critical issue for PtSn catalysts is a poor corrosive resistance in the electrochemical environment, resulting in dissolution of the non-noble component and losses in electrocatalytic performance. Therefore, a series of experiments were performed to check the corrosion and electrochemical stability of the Sn-modified smooth polycrystalline Pt electrode. These included AFM, XPS analyses and electrochemical studies of the surface composition after the immersion of Sn-modified Pt into 0.5-M sulfuric acid solution under open-circuit conditions. Electrocatalytic activity of Pt surfaces modified by spontaneously deposited tin species in electrooxidation of C-1 molecules (carbon monoxide, formaldehyde, formic acid and methanol) will be demonstrated in a forthcoming publication [68].

## Materials and methods

The solution of $H_2SnCl_4$ (ca. 3.5 M) was freshly prepared by dissolving $SnCl_2{\cdot}2H_2O$ in concentrated HCl to avoid hydrolysis of tin chloride. A spontaneous modification of the clean polycrystalline Pt foil surface was carried out by (i) immersing the sample into $SnCl_2$/HCl solution under open-circuit conditions at room temperature for 2 min, and (ii) subsequent extensive rinsing of the sample by pure water. All procedures were performed at ambient temperatures under a naturally aerated environment. After drying the surface in a stream of Ar gas (from Elmemesser, 99.999%) the sample was used for AFM, XPS or electrochemical measurements respectively either directly, or after additional treatment in 0.5-M $H_2SO_4$ for 15 min under open-circuit conditions, followed by corresponding washing/drying. Analytical grade chemicals and triply distilled water were used to prepare the solutions.

The AFM measurements were carried out using an atomic probe microscope Explorer Topometrix (USA) in a non-contact mode. The XPS analyses were performed on a spectrometer ESCALAB-MKII VG Scientific (UK) equipped with Mg $K_\alpha$ X-ray radiation source (300 W) and $Ar^+$ ion gun (20 $\mu A/cm^2$).

The cyclic voltammograms were recorded using a computerized potentiostat PI-50-1 and a function generator PR-8 (Russia) in a standard three-electrode electrochemical cell in 0.5-M $H_2SO_4$ solution purged by Ar. The working electrode was Pt foil of 2 $cm^2$ (1×1 cm) geometric area (real surface area, determined from hydrogen-UPD charge [69, 70, 71], 6.8 $cm^2$), the counter electrodewas a Pt sheet of ca. 2 $cm^2$ area (1×1 cm) and the reference electrode was $Ag/AgCl/KCl_{sat.}$(all potentials are quoted vs. a Standard Hydrogen Electrode, SHE).

## Results

### AFM characterization of tin-modified Pt surface

Surface imaging by means of AFM was used for comparative studies of the morphology of (i) clean polycrystalline platinum, (ii) Pt modified by spontaneous deposition/hydrolysis of tin species from acidic tin chloride solution under open-circuit conditions as described in the section Materials and methods, and (iii) Sn-modified Pt etched in sulfuric acid solution under open-circuit conditions. Figure 1 shows corresponding AFM images of mirror-polished polycrystalline Pt (Fig. 1a–c), tin-modified Pt (Fig. 1d–f) and Sn-modified Pt after 10 min treatment in 0.5-M $H_2SO_4$ (Fig. 1g–i). For each case representative areas of the surface were

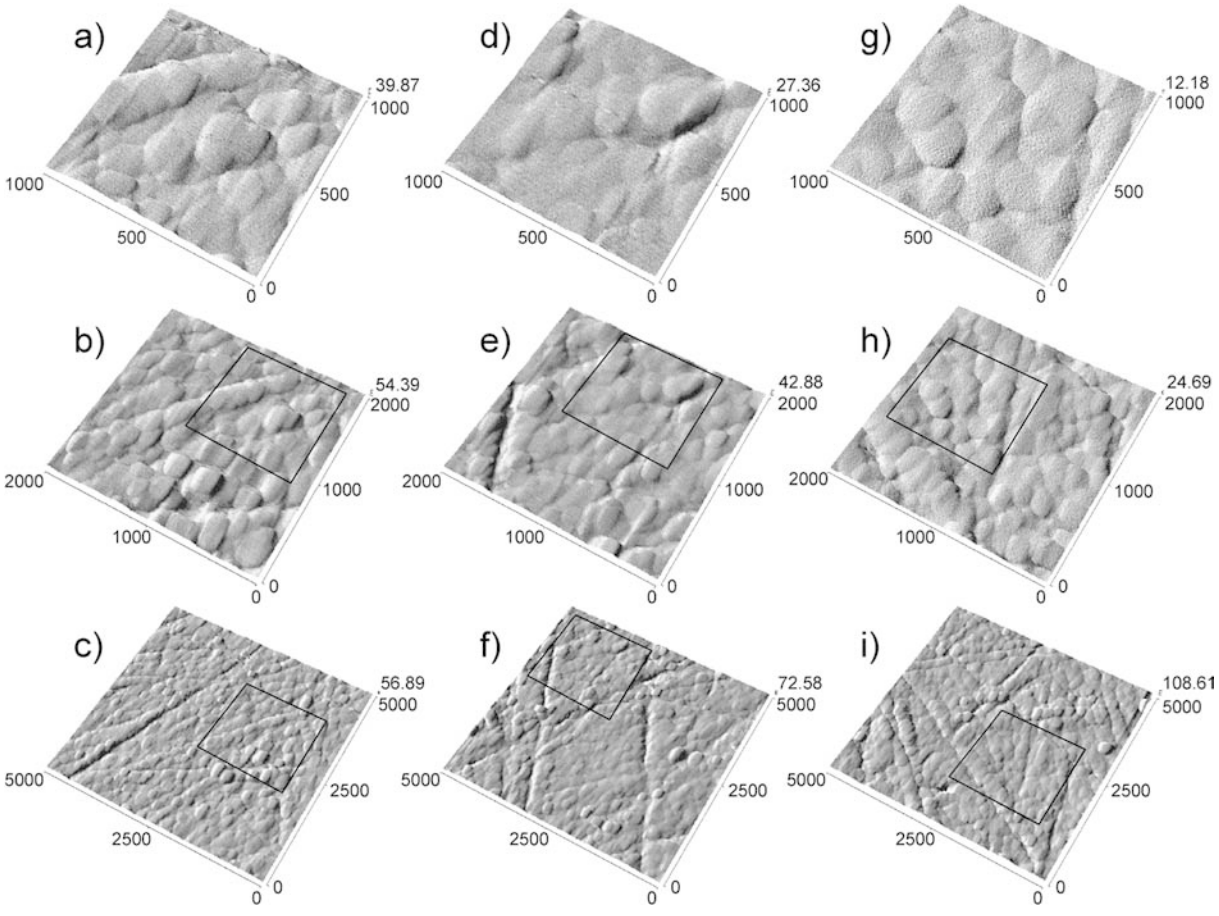


**Fig. 1** Representative atomic force microscopy images (in nm) for the clean mirror-polished polycrystalline Pt surface (**a**–**c**), after spontaneous modification of a Pt surface by Sn species (**d**–**f**), and Sn-modified Pt surface after etching in 0.5-M $H_2SO_4$ solution (**g**–**i**). Zoomed areas are highlighted accordingly

randomly selected (5,000×5,000 nm) and zoomed in to higher magnification (up to 1,000×1,000 nm).

A clean polycrystalline Pt surface exhibits a domain morphology, consisting of rectangular overlapping crystallite facets 100–200 nm in width and length, and 40–60 nm in height (Fig. 1a–c). Such a faceted surface is formed after polishing a Pt disk to mirror grade with a diamond paste up to 0.1-μm grain size (note polishing traces in images of lower magnification), subsequent degreasing in methanol and a freshly prepared hot mixture of concentrated sulfuric acid and hydrogen peroxide, extensive rinsing with pure water, and, finally, repetitive cycling in the potential window between hydrogen and oxygen bulk evolution in deaerated 0.5-M $H_2SO_4$ solution to obtain a stable CV, corresponding to a voltammetric response of clean polycrystalline Pt electrode [71]. The latter treatment is known to induce a mobility in Pt surface atoms leading to faceting and structuring of the surface [72, 73, 74].

The tin-modified Pt surface images (Fig. 1d–f) show several differences compared to clean Pt (Fig. 1a–c) (note that due to ex situ modification the AFM images display different areas of the surface before and after modification). The shape of tin-modified crystallites becomes more ''rounded'' (Fig. 1d–f) compared to rectangular domains on a clean polycrystalline Pt surface (Fig. 1a–c). The fine structure of the lower height crystallites becomes ''smoothed'' and less clearly resolved as could be seen from the comparison of corresponding images at each magnification: the height of the crystallites on the Sn-modified surface becomes lower as seen in higher magnification images (for low magnification images such a comparison is rather complicated due to large differences in the topology as a result of higher number of polishing traces of a different depth, and crystallite structures of a different height, at different locations on Pt surface). On the other hand the underlying structures of Pt crystallites can still be clearly resolved on the Sn-modified Pt surface, and the presence of new structural features can be hardly distinguished at higher magnification (Fig. 1d), in agreement with in situ scanning tunneling microscopy findings for a tin-UPD modified Pt(111) surface at even higher resolution [45]. Overall, the absence, rather than presence, of the new features (occurrence of new crystallites, dendrites or islands, which would suggest new phase growth) after modification at a given AFM magnification, in combination with a clear evidence of the presence of the resulting modifying Sn species on Pt surface (see XPS and CV data in the sections XPS characterization of tin-modified Pt surface and Electrochemical characteriza-

tion of tin-modified Pt surface) strongly suggest that a thin and uniform layer of tin species is formed after spontaneous modification of Pt surface.

For the acid-etched Sn-modified Pt surface (Fig. 1g–i) the underlying Pt crystallite structure becomes better resolved compared to Sn-modified Pt (Fig. 1d–f) though still not as clear as that for a clean Pt surface (Fig. 1a–c) according to representative AFM images at all magnifications. The topography of the surface becomes smoother than Sn-modified Pt, as can be judged from the images at higher magnifications. Moreover, at higher magnifications the occurrence of the ill-resolved nano-sized features can be visualized over the crystallites surface for the acid-etched Sn-modified Pt. Due to the rather inert nature of the substrate material (polycrystalline Pt) against the exposure to a moderately acidic solution (0.5-M sulfuric acid) under open-circuit conditions and at room temperature, such corrosion-induced features can be attributed to the selective dissolution of the modifying film rather than the substrate. This can be rationalized in terms of a different stability of the film components in acidic medium, leading to preferential dissolution of certain species constituting the film and resulting in variations in composition of the modifying film as will be discussed further.

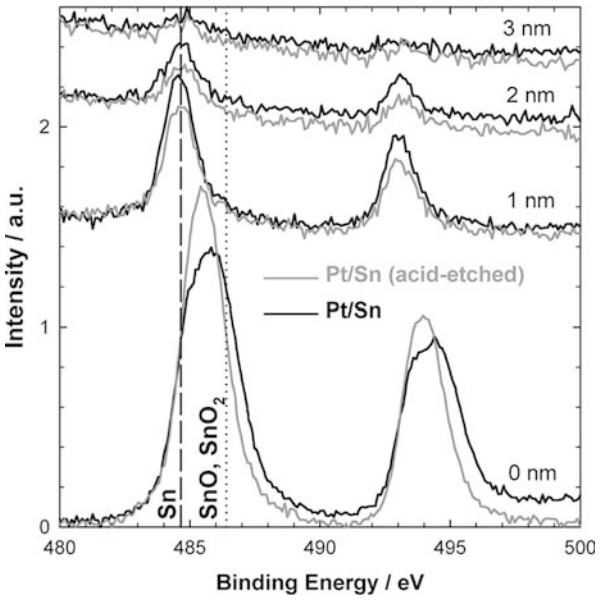


**Fig. 2** X-ray photoelectron spectra depth profiles for Sn 3d region of an Sn-modified Pt surface before (*black*) and after (*gray*) etching in 0.5-M $H_2SO_4$ solution

## XPS characterization of tin-modified Pt surface

To get further qualitative and quantitative information on the composition of the modifying film, XPS analyses of the tin-modified surface before and after treatment in sulfuric acid solution were carried out. Due to the ex situ sample preparation procedure and an exposure to the atmosphere during a sample transfer to the XPS chamber, the spectra were recorded not only from the sample surface, but also depth-profile spectra were taken after $Ar^+$ sputtering to get a deeper insight into the composition of the modifying layer.

The XP spectra of tin-modified mirror-polished polycrystalline platinum (Fig. 2, black line) confirm the presence of tin species on the Pt surface after the spontaneous modification procedure described above, as evidenced from the peak doublet characteristic of tin species [75]. The asymmetric shape of the peaks suggests the presence of at least two types of tin species on Pt surface based on the binding energy ($E_b$) of Sn $3d_{5/2}$ electrons—the binding energy $E_b = 486.4$ eV corresponds to tin oxide(s)/hydroxide(s), while $E_b = 484.65$ eV can be attributed to metallic tin [75], in agreement with the XPS analysis of UHV-prepared well-characterized Pt(111)Sn ordered surface alloys oxidized in an oxygen atmosphere [76]. The acid-etched tin-modified Pt sample exhibits a lower amount of tin species at the surface (gray line) compared to the untreated sample (black line), as evidenced from the narrowing of the peak width at higher binding energies and the peak shift to lower BE values for the acid-etched sample (ca. 485.5 eV, corresponding to "quasimetallic" Sn [76]). Therefore, it might be assumed that the acid-etch treatment results in a preferential dissolution of less stable oxidized tin species, apparently, tin hydroxy species developed most likely due to hydrolysis of tin chlorocomplex upon rinsing with water. This assumption is supported by our AFM data (see previous section, AFM characterization of tin-modified Pt surface), and the literature data about the corrosion stability and composition of anodically pre-formed passive films on tin [77, 78].

As already mentioned, due to the ex situ preparation procedure and atmospheric exposure during transfer of the sample, the XPS analysis of the Sn-modified Pt topmost layer can hardly provide any direct evidence about the oxidation state of the modifying tin species. Furthermore, even for the anaerobic back-transfer experiments for the UHV-prepared well-characterized Pt(111)Sn surface alloys, a partial oxidation of tin sites cannot be avoided due to the potential control loss upon emersion of the surface [32]. Therefore, we performed a depth-profile XPS analysis for the tin-modified Pt surfaces before and after etching in 0.5-M $H_2SO_4$to investigate their composition and corrosion stability.

The sputtering of the surface by $Ar^+$ ions (Fig. 2) results in a gradual decrease in intensity of corresponding peaks and their shift to lower binding energy values, suggesting an overall loss of the modifying species from the surface due to $Ar^+$ ion bombardment and a comparative enrichment of the residual layer by the metallic tin component. A presence of tin metal in the modifying adlayer is clearly evidence for Sn-modified Pt before and after etching in 0.5-M $H_2SO_4$ indicating (i) formation of tin metal on the Pt surface upon spontaneous modification in $SnCl_2$/HCl solution under open-

circuit conditions; (ii) a satisfactory stability of modifying tin layer upon exposure to acidic solution. The decrease in the XPS peak intensities for tin species down to nearly background level after 1.5 min of $Ar^+$ etching at the rate ca. 2 nm/min suggests that the thickness of the modifying layer does not exceed 2–3 nm—the residual tin amount after etching up to 3 nm depth can be attributed to tin species located in the gaps of the underlying Pt surface, taking into account the roughness of Pt substrate (see Fig. 1). The Pt $4f_{7/2}$ spectra sputter profiles (not shown) of corresponding tin-modified surfaces has only slight variation in the peak doublet intensity and the binding energy with the sputter time (depth) corresponding to Pt metal ($E_b = 70.9$ eV) [75].

Finally, the overall elemental composition of the Sn-modified Pt surface upon $Ar^+$ sputter before and after acid etching was determined from the peak area for the XP spectra for Sn 3d (both metallic and oxidic), Pt 4f, O 1s, Cl 2p and S 2p taking into account the sensitivity factor for each element (Table 1). The spontaneously modified Pt/Sn surface is enriched by oxygen species (ca. 56 at%), contains about equal amounts (ca. 20 at%) of Pt and Sn (both metallic and oxidized) and about 5 at% of Cl (the latter comes as anion from the modifying solution). $Ar^+$ sputter before the XPS analysis results in gradual decrease of oxygen (to ca. 4 at%), Cl (down to 0 at%) content and corresponding increase in Pt content (up to 95 at%). The amount of tin species (both metallic and oxidic) first relatively increases due to a five-fold decrease in content oxygen species, prevailing at the topmost layer, and then decreases to ca. 2 at% (mainly metallic). For the acid-treated Pt/Sn surface the amount of oxygen (ca. 40 at%) and tin species (ca. 10 at%) is relatively lower, compared to untreated surface, at about twice higher Pt content (ca. 40 at%), the same amount of Cl and a small amount of sulfur (sulfate from the etching solution). $Ar^+$ sputtering for 30 s leads to about the same elemental composition of the acid-treated sample as that for an untreated Pt/Sn sample sputtered for 90 s, indicating a thinner modifying layer and prevailing metallic tin species for the first case.

## Electrochemical characterization of tin-modified Pt surface

Next we have studied the electrochemical stability of spontaneously Sn-modified Pt electrodes in 0.5-M sulfuric acid solution under controlled potential. For that the electrode was immersed at 0 V vs. SHE and held at this potential for ca. 5 min. After that the electrode potential was scanned to more positive values gradually increasing the positive limit of the potential. In this way a series of cyclic voltammograms (CVs) of the tin-modified Pt electrode were recorded in 0.5-M sulfuric acid solution (Fig. 3, solid lines) and compared with analogous CVs on clean polycrystalline Pt (Fig. 3, dotted lines). No significant difference was found in the current–voltage response for the Pt electrode directly after spontaneous modification by tin species (not shown) compared to that after additional etching in sulfuric acid solution under open-circuit conditions (Fig. 3, solid lines), suggesting negligible losses of electroactive species during the etching procedure.

Hydrogen adsorption/desorption features, typical for a clean polycrystalline Pt electrode in sulfuric acid solution [71] (Fig. 3, dotted lines) are largely suppressed on Sn-modified Pt electrode in the potential region 0–0.3 V (SHE) confirming the presence of tin species on the Pt surface (Fig. 3, solid lines). Correspondingly, the pseudo-capacitive current in the double-layer region is increased due to adsorption/desorption of OH species on Sn sites. The CV of Sn-modified Pt shows reproducible current–voltage traces in the potential window 0–0.6 V (SHE) in accordance with the literature data for Sn-UPD-modified Pt electrodes [35, 36, 37, 38, 39, 40, 41, 42, 43, 44, 45, 46], suggesting that the modifying tin species are relatively stable in this potential window.

**Table 1** XPS analysis of the elemental composition of modifying layer after spontaneous deposition of tin species onto Pt surface, and that after etching the modifying layer in 0.5 M $H_2SO_4$ solution

| $Ar^+$ sputter time (s) ($\sim$2 nm $min^{-1}$) | Element | Composition (at%) | $E_b$ (Sn $3d_{5/2}$) (eV) | Composition (at%) | $E_b$ (Sn $3d_{5/2}$) (eV) |
|---|---|---|---|---|---|
| | | Sn-modified Pt | | Acid-etched Sn-modified Pt | |
| 0 | Pt | 20.98 | 486.3 and 484.9 | 43.30 | 485.4 and 485.9 |
| | O | 56.21 | | 39.78 | |
| | Sn | 18.07 | | 11.01 | |
| | Cl | 4.74 | | 4.82 | |
| | S | 0 | | 1.09 | |
| 30 | Pt | 62.28 | 484.8 and 485.8 | 94.50 | 484.6 |
| | O | 11.68 | | 2.36 | |
| | Sn | 23.22 | | 3.14 | |
| | Cl | 2.82 | | 0 | |
| | S | 0 | | 0 | |
| 90 | Pt | 94.59 | 484.6 | 96.90 | 484.6 |
| | O | 3.656 | | 2.48 | |
| | Sn | 1.75 | | 0.62 | |
| | Cl | 0 | | 0 | |
| | S | 0 | | 0 | |

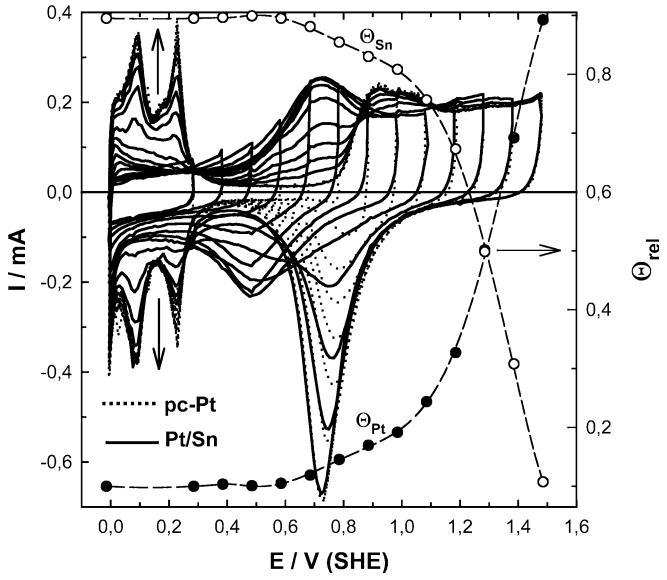


**Fig. 3** Cyclic voltammograms for a clean polycrystalline Pt surface (*dotted lines*) and an Sn-modified surface etched in 0.5-M $H_2SO_4$ solution (*solid lines*), and a coverage of Pt (filled circles) and Sn (open circles) as a function of the positive potential limit. 0.5 M $H_2SO_4$, $v = 50$ mV/s, $t = 20$ °C

After excursions to potentials more positive 0.6 V, hydrogen adsorption/desorption peaks, characteristic for polycrystalline Pt, start to develop indicating a decrease in tin coverage due to anodic dissolution of tin species. The relative Sn-free Pt coverage ($\Theta_{Pt}$), quantified for each cycle from the ratio of hydrogen adsorption charge on Sn-modified surface ($Q_{H(Pt/Sn)}$) to that on pure Pt ($Q_{H(Pt)}$) as $\Theta_{Pt} = Q_{H(Pt/Sn)}/Q_{H(Pt)}$, is plotted in Fig. 3 (filled circles). The calculated coverage of Sn-free Pt sites is about 0.1 up to a potential of 0.6 V, followed by a nearly linear increase to 0.2 coverage at 1.0 V, and then increases rapidly up to 0.9 at 1.5 V. (Please note that for calculation of the absolute coverage value the relative coverage should be corrected by 0.77 corresponding to H-UPD coverage on polycrystalline Pt at the onset of bulk hydrogen evolution [70].) Correspondingly, the relative coverage of tin species ($\Theta_{Sn}$), found as $\Theta_{Sn} = 1 - Q_{H(Pt/Sn)}/Q_{H(Pt)}$ and plotted in Fig. 3 (open circles), mirrors the dependence of $\Theta_{Pt}$ on the electrode potential and agrees well with the data reported in the literature for the underpotentially pre-formed tin adlayers on Pt electrodes [35, 36, 47].

With an increase in the potential limit more positive H-UPD region ($> 0.3$ V) a pair of quasi-reversible redox peaks starts to develop for Sn-modified surface in concert with simultaneous development of the H-UPD features on Pt, when passing the positive potential limit of 0.6 V (Fig. 3, solid lines). Corresponding redox peaks for Sn-modified electrode are centered at ca. 0.72 V in the positive-going scan and about 0.48 V in the negative-going scan, characteristic for Sn-UPD-modified Pt surfaces [35, 36, 37, 38, 39, 40, 41, 42, 43, 44, 45, 46]. These peaks are usually attributed to the Sn(II)/Sn(IV) redox couple for tin oxide/hydroxide species immobilized onto a Pt surface according to ex situ (XPS [14, 32, 42]) and in situ (radiotracer [35], Raman spectroscopy [37]) characterization of the Sn-UPD layers on Pt surfaces. The charge corresponding to the anodic peak of tin species oxidation, calculated within the potential range 0.3–0.9 V as the difference between positive-going scans for tin-modified and clean polycrystalline Pt respectively, is ca. 0.2 mC $cm^{-2}$, i.e., similar to hydrogen adsorption charge on polycrystalline Pt (0.21 mC $cm^{-2}$ [69]). Assuming two electrons are involved in tin species redox process, this suggests ca. two Sn atoms per Pt site in agreement with previous findings for Sn-UPD on polycrystalline Pt [35, 36, 42, 64].

Anodic oxidation of tin metal to Sn(II) hydroxide ($OH^-$ adsorption on Sn sites) most likely occurs more negative 0.3 V, according to recent detailed study on ultrahigh vacuum prepared and characterized Pt(111)Sn electrodes [31, 32], as concluded from the early onset (ca. 0.2 V) for adsorbed [32] and bulk [31] CO oxidation on these surfaces. In a recent electrochemical quartz crystal microbalance study the above mentioned redox peaks for the Sn-UPD-modified Pt surface were attributed to four-electron oxidation/reduction of metallic tin to Sn(IV) hydroxide/oxide [46]. A drastic decrease in the tin species coverage at potentials more positive 1.0 V (Fig. 3, white circles) corresponding to a small anodic current peak in PtO region (Fig. 3, solid lines) can be explained by oxidation of a tin fraction forming a surface alloy [42] and removal of a tin oxide species from the surface due to PtO formation.

## Discussion

The presence of metallic tin in the modifying layer strongly suggests that a Sn(II) tetrachloro-complex, formed due to dissolution of tin chloride in concentrated hydrochloric acid (see [79] and references cited therein)

$$SnCl_2 + 2\,HCl \rightarrow SnCl_4^{2-} + 2\,H^+ \quad (1)$$

disproportionates spontaneously to metallic tin and Sn(IV) on a Pt surface under open-circuit conditions as postulated in [64]—the reaction known as electroless tin plating and used for Sn metal deposition without applying an external current [80]:

$$2\,Sn(II) \rightarrow Sn(0) + Sn(IV) \quad (2)$$

The specific feature of this process is that electrochemical half-reactions occur simultaneously on a Pt surface under open-circuit conditions according to a mixed-potential theory [80]: an anodic reaction—oxidation of Sn(II) to Sn(IV)—and a cathodic reaction—reduction of Sn(II) to Sn metal (and/or discharge of protons to hydrogen) by electrons released in the anodic half-reaction being transferred through the Pt surface (the latter pathway requires a conductive and catalytically active substrate, such as Pt). Moreover, in strongly

acidic solution (concentrated hydrochloric acid) a growing non-noble tin deposit is partly dissolved according to the reaction

$$Sn + 2\,HCl \rightarrow SnCl_2 + H_2 \quad (3)$$

preventing continuous growth of a tin metal film (complete Pt surface blocking) and apparently resulting in the formation of metallic tin nano-structures at submonolayer amounts in accordance with AFM (Fig. 1), XPS (Fig. 2) and CV (Fig. 3) data. Evidently, the amount of metallic tin deposited is controlled by the rate of tin deposition/dissolution (reactions 2 and 3) and can be easily varied by changing concentration of $SnCl_2$ and HCl.

The formation of tin oxide/hydroxide species on a Pt surface most likely results from the hydrolysis of Sn(II) chloride complex during rinsing of the surface by water and/or aerobic exposure of the probe during the preparation and transfer to the XPS chamber. The hydrolysis of Sn(II) chloride complex resulting in tin oxide/hydroxide deposit is well known and widely used for pretreatment of dielectric material surfaces prior to activation with Pd ions and electroless deposition of desired metal and alloy films [67, 80] and can be described by the following reactions

$$SnCl_2 + 2\,H_2O \rightarrow Sn(OH)_2 + 2\,HCl \quad (4)$$

$$Sn(OH)_2 \rightarrow SnO + H_2O \quad (5)$$

However, electroless deposition of tin metal due to spontaneous disproportionation of tin tetrachlorocomplex (1–2) requires conductive and catalytically active substrate, e.g., Pt surface. In the latter case it is also possible, that tin deposition is self-inhibited when reaching a close to monolayer coverage of metallic tin, in agreement with quantitative evaluation of electrochemical measurements discussed in the section Electrochemical characterization of tin-modified Pt surface.

## Conclusions

A simple ''dip-coating'' method for Pt surface modification through spontaneous deposition of tin and tin oxy-species has been developed. It consists of Pt immersion into $SnCl_2$/HCl solution under open-circuit conditions and subsequent rinsing of the surface by pure water. The AFM and XPS results suggest that a thin (average thickness ca. 2 nm) and quite uniform layer of tin species is formed after spontaneous modification of the Pt surface. Based upon the XPS characterization, two kinds of tin species were identified on the Pt surface after modification, namely, tin oxy-compounds and metallic tin. Tin oxide/hydroxide species were derived as a result of Sn(II) chloride complex hydrolysis, while tin metal was deposited spontaneously on the Pt surface due to disproportionation of Sn(II) to Sn(IV) and metallic tin. The layer of modifying tin-species shows a satisfactory stability at potentials relevant to low-temperature fuel cell operating conditions (0–0.6 V vs. SHE). The suggested method for spontaneous Sn modification offers a large variety for tailored nano-structured fuel cell catalyst formulations, including the possibility for modification of both catalyst particles and/or carbon support.

**Acknowledgements** The authors are indebted to A. Kaliničenko for the AFM measurements. Financial support from the Lithuanian Foundation of Science and Studies through grant No. T-540 is greatly acknowledged. G.S. is most grateful for Jerome and Isabella Karle scholarship from the World Federation of Scientists.

## References

1. Watanabe M, Motoo S (1975) J Electroanal Chem 60:267
2. Watanabe M, Motoo S (1975) J Electroanal Chem 60:275
3. Markovic NM, Ross PN (2002) Surf Sci Rept 45:117
4. Gurau B, Viswanathan R, Liu R, Lafrenz TJ, Ley KL, Smotkin ES, (1998) J Phys Chem B 102:9997
5. Reddington E, Spienza A, Gurau B, Viswanathan R, Sarangapani S, Smotkin ES, Mallouk TE (1998) Science 280:1735
6. Reetz MT, Lopez M, Grünert W, Vogel W, Mahlendorf F (2003) J Phys Chem B 107:7414
7. Petry OA, Podlovchenko BI, Frumkin AN, Lal H (1965) J Electroanal Chem 10:253
8. Iwasita T, Nart FC, Vielstich W (1990) Ber Bunsen-Ges Phys Chem 94:1030
9. Jusys Z, Massong H, Baltruschat H (1999) J Electrochem Soc 146:11093
10. Iudice de Souza JP, Iwasita T, Nart FC, Vielstich W (2000) J Appl Electrochem 30:43
11. Habble CT, Wrighton MS (1991) Langmuir 7:1305
12. Gonzales MJ, Hable CT, Wrighton MS (1998) J Phys Chem B 102:9881
13. Cathro KJ (1969) J Electrochem Soc 116:1608
14. Andrew MR, Druby JS, McNicol BD, Pinnington C, Short RT (1976) J Appl Electrochem 6:99
15. Watanabe M, Uchida M, Motoo S (1987) J Electroanal Chem 229:395
16. Boennemann H, Richards RM (2001) Eur J Inorg Chem 2460
17. Roth C, Martz N, Hahn F, Leger JM, Lamy C, Fuess H (2002) J Electrochem Soc 149:E433
18. Dickinson AJ, Carrette LPL, Collins JA, Friedrich KA, Stimming U (2002) Electrochim Acta 47:3733
19. Schmidt TJ, Gasteiger HA, Behm RJ (1999) J New Mater Electrochem Systems 2:27
20. Manzo-Robledo A, Boucher AC, Pastor E, Alonso-Vante N (2002) Fuel Cells 2:109
21. Watanabe M, Zhu Y, Uchida H (2000) J Phys Chem B 104:1762
22. Igarashi H, Fujino T, Zhu Y, Uchida H, Watanabe M (2001) Phys Chem Chem Phys 3:306
23. Uchida H, Ozuka H, Watanabe M (2003) Electrochim Acta 47:3629
24. Gasteiger HA, Markovic NM, Ross PN, Cairns EJ (1993) J Phys Chem 97:12020
25. Gasteiger HA, Markovic NM, Ross PN, Cairns EJ (1994) J Phys Chem 98:617
26. Gasteiger HA, Markovic NM, Ross PN, Jr (1995) J Phys Chem 99:8945
27. Wang K, Gasteiger HA, Markovic NM, Ross PN (1996) Electrochim Acta 41:2587
28. Grgur BN, Zhuang G, Markovic NM, Ross PN, Jr (1997) J Phys Chem B 101:3910
29. Grgur BN, Markovic NM, Ross PN (1999) J Electrochem Soc 146:1613

30. Ross PN, Jr (1998) The science of electrocatalysis on bimetallic surfaces. In: Lipkowski J, Ross PN (eds) Electrocatalysis, chapter 2. Wiley-VCH, Heidelberg, pp 43–74
31. Stamenkovic VR, Arenz M, Lucas CA, Gallagher ME, Ross PN, Markovic NM (2003) J Am Chem Soc 125:2736
32. Hayden BE, Rendall ME, South O (2003) J Am Chem Soc 125:7738
33. Janssen MMP, Moolhuysen J (1976) Electrochim Acta 21:861
34. Motoo S, Shibata M, Watanabe M (1980) J Electroanal Chem 110:103
35. Sobkowski J, Franaszczuk K, Piasecki A (1985) J Electroanal Chem 196:145
36. Bittins-Cattaneo B, Iwasita T (1987) J Electroanal Chem 238:151
37. Holze R, Bittins-Cattaneo B (1988) Electrochim Acta 33:353
38. Beden B, Kadirgan F, Lamy C, Leger JM (1981) J Electroanal Chem 127:75
39. Norton Hanner A, Ross PN (1991) J Phys Chem 95:3740
40. Morimoto Y, Yeager EB (1998) J Electroanal Chem 444:95
41. Morimoto Y, Yeager EB (1998) J Electroanal Chem 444:100
42. Lamy-Pitara E, El Quazzani-Benhima L, Barbier J, Cahoreau M, Caiso J (1994) J Electroanal Chem 372:233
43. Xia H (1999) Electrochim Acta 45:1057
44. Massong H, Tillmann S, Langkau T, Abd el Meguid EA, Baltruschat H (1998) Electrochim Acta 44:1379
45. Xiao XY, Tillmann S, Baltruschat H (2002) Phys Chem Chem Phys 4:4044
46. Santos MC, Bulhoes LOS (2003) Electrochim Acta 48:2607
47. Vassiliev YB, Bagotzky VS, Osetrova VN, Mikhailova AA (1979) J Electroanal Chem 97:63
48. Berenz P, Tillmann S, Massong H, Baltruschat H (1998) Electrochim Acta 43:3035
49. Massong H, Wang H, Samjeske G, Baltruschat H (2000) Electrochim. Acta 46:701
50. Crabb EM, Marshall R, Thompsett D (2000) J Electrochem Soc 147:4440
51. Crabb EM, Ravikumar MK (2001) Electrochim Acta 46:1033
52. Kaiser J, Jusys Z, Behm RJ, Moertel R, Boennemann H (2001) In: 1st European PEFC Forum. Proceedings. Lucerne, Switzerland, pp 59–62
53. Gonzales MJ, Peters CH, Wrighton MS (2001) J Phys Chem B 105:5470
54. Vavilova VV, Vasina SY, Safonova TY, Perii OA (1988) Electrokhimiya 24:1141
55. Hoster H, Iwasita T, Baumgärtner H, Vielstich W (2001) Phys Chem Chem Phys 3:337
56. Davies JC, Hayden BE, Pegg DJ, Rendall ME (2002) Surf Sci 496:110
57. Chrzanowski W, Wieckowski A (1997) Langmuir 13:5974
58. Tremiliosi-Filho G, Kim H, Chrzanowski W, Wieckowski A, Grzybowska B, Kulesza P (1999) J Electroanal Chem 467:143
59. Friedrich KA, Geyzers KP, Marmann A, Stimming U, Vogel R (1998) Z Phys Chem 208:137
60. Lin WF, Zei MS, Eiswirth M, Ertl G, Iwasita T, Vielstich W (1999) J Phys Chem B 103:6968
61. Crown A, Moraes IR, Wieckowski A (2001) J Electroanal Chem 500:333
62. Friedrich KA, Geyzers KP, Dickinson AJ, Stimming U (2002) J Electroanal Chem 524–525:261
63. Samjeske G, Xiao XY, Baltruschat H (2002) Langmuir 18:4659
64. Szabo S (1984) J Electroanal Chem 172:359
65. Campbel SA, Parsons R (1992) J Chem Soc Faraday Trans 88:833
66. Waszczuk P, Solla-Gullon J, Kim HS, Tong YY, Montiel V, Aldaz A, Wieckowski A (2001) J Catal 203:1
67. Liu Z, Lin X, Lee JY, Zhang W, Han M, Gan LM (2002) Langmuir 18:4054
68. Stalnionis G, Tamašauskaitė-Tamašiūnaitė L, Pautienienė V, Jusys Z (2004) J Solid State Electrochem, in press
69. Bagotzky VS, Vassiliev YB, Khazova OA (1977) J Electroanal Chem 81:229
70. Biegler T, Rand DAJ, Woods R (1971) J Electroanal Chem 29:269
71. Angerstein-Kozlowska H, Conway BE, Sharp WBA (1973) J Electroanal Chem 43:9
72. Cervino RM, Tracia WE, Arvia AJ (1985) J Electrochem Soc 132:266
73. Cervino RM, Arvia AJ, Vielstich W (1985) Surf Sci 154:623
74. Zinola CF, Bello C (2003) J Colloid Interface Sci 258:259
75. Wagner CD, Riggs WM, Davis CE, Moulder JS, Muilenberg GE (eds) (1979) In: Handbook of X-ray photoelectron spectroscopy. Perkin Elmer, Eden Praire, Minn.
76. Jerdev DI, Koel BE (2001) Surf Sci 492:106
77. Moina CA, Ybarra GO (2001) J Electroanal Chem 504:175
78. Šeruga M, Metikoš-Hukovic M, Valla T, Milun M, Hoffschultz H, Wandelt K (1996) J Electroanal Chem 407:83
79. Mandler D, Bard AJ (1991) J Electroanal Chem 307:217
80. Mallory GO, Hajdu B (eds) (1996) In: Electroless plating. Fundamentals and applications. American Electroplating Soc, Orlando, Fla.